

Geological and geochemical characteristics of basalts from Hardat Tolgoi Mine, Inner Mongolia, China

XU Hui^{1,2}, CHEN Jinquan³, and LU Zhaohua^{1*}

¹ School of Chemical and Environmental Engineering, China University of Mining & Technology, Beijing 100083, China

² Shandong Provincial Engineering and Technology Research Center for Wild Plant Resources Development and Application of Yellow River Delta, Binzhou University, Binzhou 256603, China

³ State Key Laboratory of Mineral Deposit Research, School of Earth Sciences and Engineering, Nanjing University, Nanjing 210093, China

* Corresponding author, E-mail: xuhui380@126.com

Received June 30, 2013; accepted November 6, 2013

© Science Press and Institute of Geochemistry, CAS and Springer-Verlag Berlin Heidelberg 2014

Abstract Basalts from Hardat Tolgoi Mine were studied systematically by using petrochemical and isotope geochemical methods in order to discuss their chemical properties, diagenetic material sources and tectonic environment. The analysis results indicate that the alkali basalts are characterized by low silica and high alkaline (Na>K) and iron-titanium contents. The distribution patterns of the rare earth elements (REE) are the "rightist" type, which typically show evident fractionation between light REEs and heavy REEs with (La/Yb)_N ratios from 8.04 to 10.4, but no significant negative Eu anomalies were observed ($\delta\text{Eu}=1.01$ to 1.04). The basalts are relatively enriched in large ion lithophile elements (LILE, Ba, Sr) and high field strength elements (HFSE, Nb, Ta, Hf). Ratios of $^{206}\text{Pb}/^{204}\text{Pb}$ vary between 18.434 and 18.550, ratios of $^{207}\text{Pb}/^{204}\text{Pb}$ are between 15.541 and 15.569, and ratios of $^{208}\text{Pb}/^{204}\text{Pb}$ are between 38.331 and 38.536. The diagenetic substance is believed from the asthenospheric mantle and in intraplate environment, which was constructed during continent stretch, without being significantly contaminated by crustal materials.

Key words petrochemistry; isotopes; basalt; Tolgoi Mine; Inner Mongolia

1 Introduction

Hardat Tolgoi lead-zinc deposit is located in the central-northern part of Xilinguole area in Inner Mongolia, China to the south of the Sino-Mongolia boundary. It is about 35 km away from the Baiyintuga of the Abaga County in southeastern part. Its GPS geographical coordinates are $114^{\circ}21'00''$ E and $45^{\circ}05'30''$ N. In regional tectonic setting, it is located in the middle of Inner Mongolia curved fold belt at the intersection of the Siberian Craton and the North China Craton, and between the Wunu'er-Erlunchun fault and the Erlianshan-Hegenshan fault (Fig. 1). It is a medium-sized lead-zinc deposit found by the Henan Nonferrous Metal Bureau of Geology and Mineral

Resources (Zhang, 2010). Basic geological research has been carried out by some predecessors. Although there has been some reference value for further study in this area (Zhang, 2010; Liu and Xu, 2003; Nie et al., 2004; Zhang et al., 2003; Wang et al., 2010; Chen et al., 2012), previous research only focused on Hadat Tolgoi lead-zinc deposit and magmatic rocks associated with the deposit. Inadequate attention has been paid to widely occurred the Cenozoic basalts outcropped near the mines. Although some basalts have been studied in the territory of Abagaqi County in Inner Mongolia (Zhang et al., 2004, 2006), due to the wide distribution of the Cenozoic basalts in the large area of Abagaqi County as well as in eastern Inner Mongolia, it is still difficult to constrain the origin of

the Cenozoic basalts in the eastern Inner Mongolia. On the basis of geological field work, we investigated the origin of basalts in and around Hadat Tolgoi mine by using whole-rock geochemistry and isotope geochemistry analyses, such as major elements, trace elements, rare earth elements and Pb isotopes analysis. Geochemical property of the basalts, metallogenic material sources and tectonic environment were identified to provide further understanding of the origin of the Cenozoic basalts in Inner Mongolia.

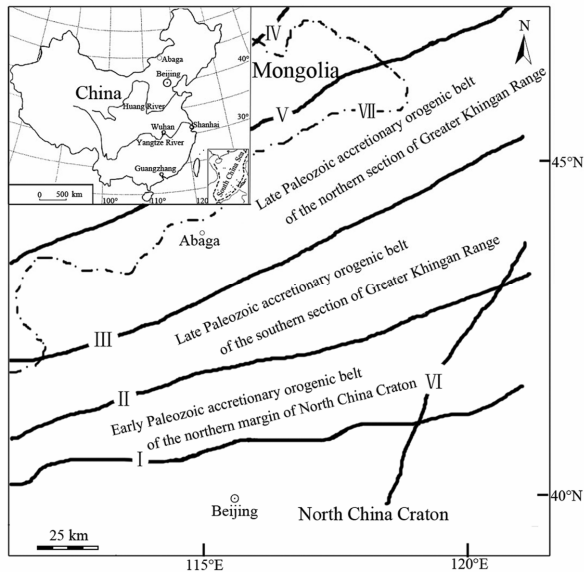


Fig. 1. Tectonic sketch map of Daxing'anling region. I. Faults on northern edge of the North China Craton; II. Xilamulun River fault; III. Erlian-Hegenshan fault; IV. Wunu'er-Elunchun fault; V. De'erbugan fault; VI. Nenjiang fault; VII. the Sino-Mongolia boundary.

2 Geology

The exposed strata in the study area include the lower Devonian Aobaoting Hundi Formation (D_{1a}), the lower Permian Baolige Formation (P_1b) and the Quaternary (Q). Major lithologies of Aobaoting Hundi Formation are gray metamorphic muddy feldspathic sandstone, metamorphosed siltstone and slate. The Baolige Formation includes upper and lower parts: lithology of the lower part (P_1b^1) is a set of dark gray carbonaceous silty slate, sandstone, dacite and lithic cuttings and crystal tuff, rhyolite and conglomerate, while the lithology of the upper part (P_1b^2) consists of a set of gray-green dacitic volcanic clastic rocks and a small amount of flow rhyolitic tuff. Lithology of the Quaternary is moraine and alluvial gravel layers. Fold structures belong to northwestward wing of Chaidamu anticlinorium with a total tendency of south to southeast direction. Major trend of fault structure is NE followed by the trend of NW. Basalts are outcropping in the surface (β) (Fig. 2a). Dikes develop well in the

mine. Granite-porphry dyke, quartz porphyry dikes, andesitic porphyry dikes and lamprophyre mainly developed in this area from Indosinian to Yanshanian period (Zhang, 2009). Most of the dikes have the trend of NW, while a few have the trend of NE. The intrusive rocks are mainly granite and diabase with hidden ore bodies. Magmatic rocks which have close relation with lead-zinc mineralization are Yanshanian granites.

3 Sampling and analytical methods

Samples were mainly collected from Hardat Tolgoi mine. Specific locality for each sample is showed in Table 1 (Fig. 2b). According to characteristics of hand specimens and thin-section observations under microscope, we selected the fresh samples and crushed them to under 200-mesh powder. Several measurements and analyses were carried out on these samples.

Analyses on major, trace and rare earth elements of the samples were conducted at the State Key Laboratory of Mineral Deposit Research at Nanjing University. Major elements were determined by using JY38S single-channel scanning high frequency Inductively Coupled Plasma Atomic Emission Spectrometer (ICP-AES). The detection limit was in the range of 0.01×10^{-6} – 0.1×10^{-6} , and the relative standard deviation (RSD) was lower than 2%. FeO was measured by using wet chemistry analysis method, and RSD was 0.5%–1%. Trace elements and rare earth elements were determined by using Finnigan Element II Inductively Coupled Plasma Mass Spectrometer (ICP-MS). The detection limit was lower than 0.5×10^{-9} , and RSD was lower than 5% (Gao et al., 2003).

Pb isotope analysis was conducted at the Research Center of Beijing Geological Institute of Nuclear Industry. Whole rock samples were decomposed by using three acid solutions, and then lead was separated with resin exchange. After the samples being dried out, lead isotopes of each sample were determined with an MAT-261 Thermal Ionization Mass Spectrometer (TIMS). RSD for 1 μ g lead content was less than 0.05% for $^{204}\text{Pb}/^{206}\text{Pb}$ and not higher than 0.005% for $^{208}\text{Pb}/^{206}\text{Pb}$.

4 Results

4.1 Petrography

The rock samples of basalts are dark gray to black with porphyritic texture and massive structure. The phenocrysts ($30\% \pm$) are mainly composed of pyroxene ($20\% \pm$), hornblende ($10\% \pm$) and olivine ($5\% \pm$). The matrix ($60\% \pm$) is in implicit texture (Fig. 3 a, b, c, d), and mainly composed of feldspar ($60\% \pm$) and pyroxene ($5\% \pm$).

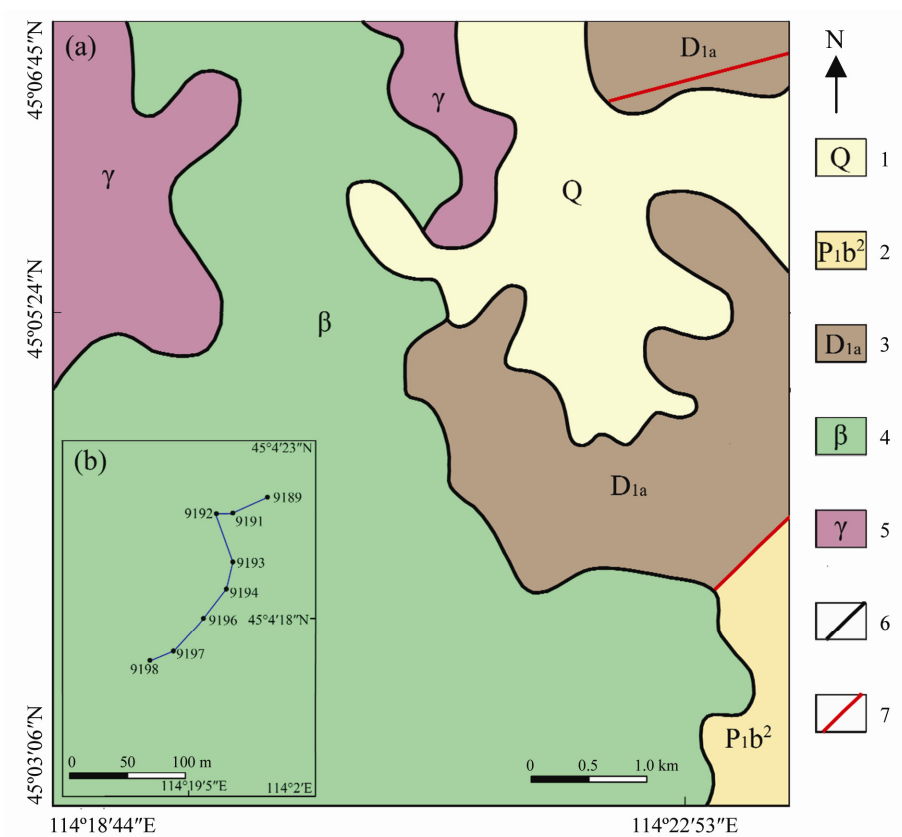


Fig. 2. Geological sketch map of Hardat Tolgoi ore district (a) and sampling localities (b). 1. The Quaternary; 2. the second section of Baolige Formation; 3. Aobaoting Hundi Formation; 4. basalt; 5. granite; 6. geological boundary; 7. fault.

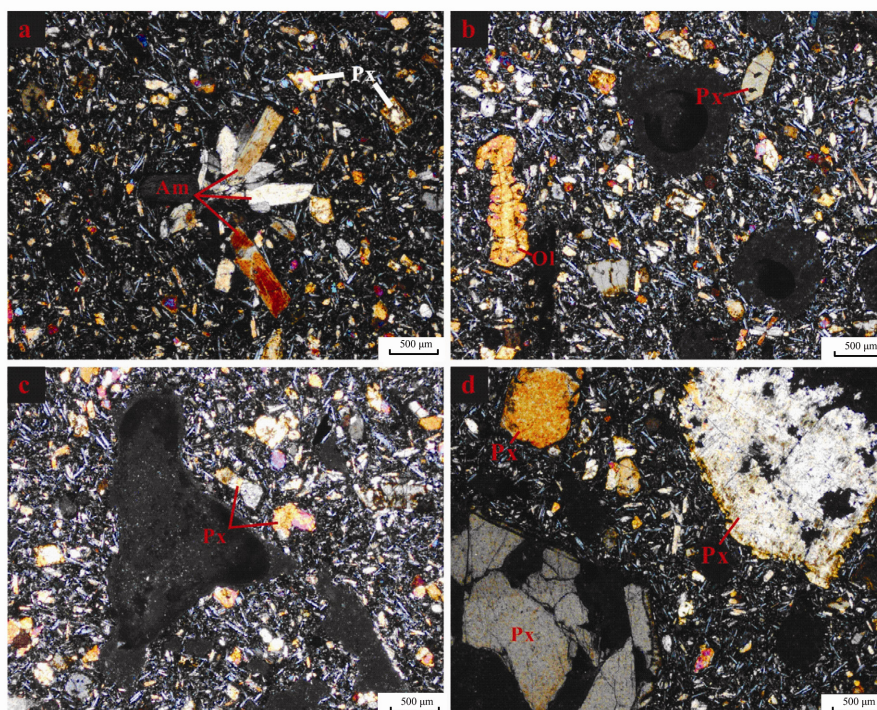


Fig. 3. Micrographs of basalt from Hardat Tolgoi ore district. Am. Amphibole; Px. pyroxene; Ol. olivine.

Table 1 Sampling locations for basalts from Hardat Tolgoi Mine

Sample	Location		Sample	Location	
9189	x:4993019	y:38526136	9194	x:4992861	y:38526065
9191	x:4992991	y:38526074	9196	x:4992799	y:38526017
9192	x:4992990	y:38526046	9197	x:4992752	y:38525974
9193	x:4992907	y:38526076	9198	x:4992735	y:38525933

Table 2 Major element contents of the alkali basalts (wt.%)

Sample	9189	9191	9192	9193	9194	9196	9197	9198
SiO ₂	46.69	46.09	43.16	44.89	44.58	45.01	44.12	43.88
TiO ₂	3.16	3.17	3.04	3.02	3.14	2.95	3.18	3.34
Al ₂ O ₃	12.44	11.96	11.12	10.78	11.21	11.73	11.02	11.06
Fe ₂ O ₃	5.37	3.32	4.57	3.44	3.41	3.02	2.97	3.45
FeO	6.90	8.77	7.66	8.66	9.14	9.32	9.57	9.72
MnO	0.19	0.16	0.17	0.17	0.18	0.17	0.17	0.18
MgO	8.12	10.14	11.66	12.09	12.86	10.10	12.84	12.22
CaO	9.60	9.01	10.40	9.43	8.80	10.15	9.36	9.27
Na ₂ O	3.02	3.26	3.06	3.17	3.19	3.13	2.98	2.84
K ₂ O	1.94	1.81	1.59	1.60	1.62	1.51	1.64	1.66
P ₂ O ₅	0.98	0.62	0.69	0.70	0.69	0.60	0.73	0.70
LOI	1.37	1.51	2.92	1.91	1.28	2.47	1.56	1.72
Total	99.78	99.82	100.04	99.86	100.10	100.16	100.14	100.04
A/CNK	0.85	0.85	0.74	0.76	0.82	0.79	0.79	0.80
A/NK	2.51	2.36	2.39	2.26	2.33	2.53	2.39	2.46
Alk	4.96	5.07	4.65	4.77	4.81	4.64	4.62	4.50
N/K	1.56	1.80	1.92	1.98	1.97	2.07	1.82	1.71
Mg [#]	55.47	60.82	64.06	64.93	65.47	60.16	65.37	63.17
σ	6.67	8.32	135.14	12.04	14.64	10.71	19.06	23.01

Table of CIPW normative mineral calculation

Or	11.66	10.89	9.68	9.66	9.70	9.14	9.84	9.99
Ab	25.33	19.25	10.01	14.95	14.19	14.94	11.52	12.70
An	14.86	12.84	12.24	10.65	11.59	13.79	11.99	12.71
Ne	0.33	4.76	9.01	6.72	7.10	6.58	7.60	6.35
Wo	11.56	12.08	15.33	13.75	11.90	14.26	12.85	12.48
En	8.86	8.32	11.55	9.79	8.45	9.45	8.93	8.66
Fs	1.47	2.76	2.21	2.71	2.39	3.76	2.83	2.78
Fo	8.24	12.22	12.93	14.74	16.86	11.48	16.54	15.69
Fa	1.50	4.47	2.73	4.51	5.27	5.04	5.78	5.56
Mt	7.91	4.90	6.82	5.09	5.00	4.48	4.37	5.09
Il	6.10	6.13	5.95	5.86	6.04	5.74	6.13	6.45
Ap	2.17	1.38	1.55	1.56	1.52	1.34	1.62	1.55

Note: State Key Laboratory for Mineral Deposit Research. Alk=Na₂O+K₂O, N/K=Na₂O/K₂O, A/CNK=Al₂O₃/(CaO+Na₂O+K₂O), A/NK=Al₂O₃/(Na₂O+K₂O) (molecule ratio), Mg[#]=100×Mg/(Mg+Fe²⁺), σ=Alk²/(SiO₂-43).

Table 3 Trace elements and rare-earth elements of alkali basalts ($\times 10^{-6}$)

Sample	9189	9191	9192	9193	9196	9198
Li	14.65	10.88	13.70	10.70	11.97	12.64
Be	2.81	2.58	2.92	2.71	2.63	2.51
Sc	16.70	17.10	16.30	15.80	17.30	17.10
Ti	20979.00	21684.60	20878.20	20676.60	20210.40	22491.00
V	187.20	181.30	178.80	174.30	183.40	192.00
Cr	263.00	247.00	313.00	295.00	228.00	308.00
Mn	1233.00	1075.00	1090.00	1084.00	1092.00	1106.00
Co	53.90	53.80	54.40	52.20	51.50	54.30
Ni	222.00	215.60	272.60	270.30	198.90	259.20
Cu	49.50	33.70	41.20	35.90	37.60	45.70
Zn	188.00	146.00	143.00	135.00	137.00	148.00
As	14.00	12.60	14.90	12.40	14.30	11.80
In	0.06	0.06	0.06	0.06	0.05	0.06
Sb	0.48	0.45	0.34	0.36	0.36	0.18
Tl	0.31	0.14	0.09	0.08	0.07	0.06
Ga	20.30	20.50	19.10	17.90	19.30	19.10
Rb	32.10	29.90	24.40	27.00	21.60	24.90
Sr	689.60	722.20	817.40	796.10	763.50	838.70
Y	47.60	44.60	42.40	40.60	40.30	42.20
Nb	61.20	62.20	67.30	64.40	55.10	69.80
Mo	2.57	2.18	2.26	2.13	1.99	2.28
Cd	0.18	0.11	0.16	0.17	0.05	0.08
Cs	1.14	0.60	1.26	0.74	0.26	0.44
Ba	405.70	386.80	425.40	403.00	405.80	449.20
Hf	12.70	12.30	11.30	10.90	10.60	11.70
Ta	4.18	4.25	4.48	4.32	3.71	4.67
Pb	5.70	9.12	9.59	6.11	5.51	5.45
Th	5.62	4.78	5.04	4.76	3.77	4.66
U	1.55	1.32	1.25	1.12	0.95	1.06
Rb/Sr	0.05	0.04	0.03	0.03	0.03	0.03
Sr/Nd	18.79	20.40	21.29	21.29	23.07	21.45
Th/U	3.63	3.62	4.03	4.25	3.96	4.40
La	38.10	35.50	39.50	37.10	31.60	39.40
Ce	70.50	66.90	72.80	68.90	59.70	72.60
Pr	9.61	9.10	10.00	9.45	8.37	10.10
Nd	36.70	35.40	38.40	37.40	33.10	39.10
Sm	10.40	9.78	10.20	9.92	9.31	10.60
Eu	3.35	3.26	3.35	3.22	3.11	3.46
Gd	9.79	9.65	9.76	9.20	8.91	9.90
Tb	2.11	1.99	2.01	1.88	1.88	2.03
Dy	12.20	11.60	11.20	10.50	10.50	11.30
Ho	2.07	1.94	1.86	1.79	1.78	1.82
Er	4.86	4.51	4.21	4.08	4.08	4.17
Tm	0.58	0.53	0.48	0.46	0.47	0.47
Yb	3.22	2.81	2.65	2.53	2.51	2.59
Lu	0.46	0.40	0.36	0.35	0.34	0.34
δEu	1.01	1.02	1.02	1.03	1.04	1.03
ΣREE	203.95	193.36	206.78	196.78	175.66	207.88
$(\text{La}/\text{Yb})_{\text{N}}$	8.04	8.58	10.13	9.96	8.55	10.33
$(\text{La}/\text{Sm})_{\text{N}}$	2.29	2.27	2.42	2.34	2.12	2.32
$(\text{Gd}/\text{Yb})_{\text{N}}$	0.76	0.76	0.74	0.79	0.73	0.74

Note: State Key Laboratory for Mineral Deposit Research; $\delta\text{Eu}=\text{Eu}_{\text{N}}/(\text{Sm}_{\text{N}}\times\text{Gd}_{\text{N}})^{1/2}$.

4.2 Major elements

Major elements compositions are listed in Table 2. Contents of SiO₂, TiO₂ and MgO in basalts are 43.16%–46.69%, 2.95%–3.34%, and 8.12%–12.86%, respectively. Alkaline content is 4.50%–5.07%, A/NK is 2.26–2.53, A/CNK is 0.74–0.85, Mg[#] is 55.47–65.47, and σ (Rittmann serial index) is 6.67–135.14. These data indicate that the basalts belong to alkaline series (mainly sodium-rich, N/K is 1.56–2.07). As showed in TAS diagram (Fig. 4), the projected points all fall above the boundary line between alkaline and subalkaline series according to Irvine et al. (1971), which also suggests the basalts belong to alkaline series. Moreover, majority of data fall in the area of basanite to basalt in the TAS diagram. According to petrography characteristics, the basalts are proved to be alkali basalts.

4.3 Rare-earth elements

Analytic results of the rare-earth elements are listed in Table 3. The value of Σ REE of the alkali basalts is 75.66×10^{-6} – 207.88×10^{-6} with an average value of 197.40×10^{-6} . Ratio of (La/Yb)_N is 8.04–10.33 with an average of 9.26; ratio of (La/Sm)_N is 2.12–2.42, with an average value of 2.29; ratio of (Gd/Yb)_N is 0.73–0.79, with an average value of 0.75; and value of δ Eu is 1.01–1.04, with an average value of 1.03. REE distribution patterns of the alkali basalts are the "rightist" type (Fig. 5a), thus the fractionation between LREE and HREE is obvious. The rare earth element distribution patterns do not appear significant negative Eu anomalies and are agree with typical alkali basalt (Li, 1992).

4.4 Trace elements

Trace element analysis results are listed in Table 3. As shown by spider diagram of trace elements in the alkali basalts (Fig. 5b), the curve is overall tilt to the right. LILE such as Ba, Sr, and HFSE such as Nb, Ta and Hf are sufficient, while HFSE Ti, Th, Y, U, and LILE Rb are deficient. Rb/Sr ratio is 0.03–0.05, close to that in primitive mantle source region (McDonough and Sun, 1995). The alkali basalts from Hardat Tolgoi mine, therefor, may have the characteristics of primitive basalts. Various trace elements of the alkali basalt from Hadat Tolgoi mine are from primitive mantle.

4.5 Lead isotopes

As presented by whole-rock lead isotope analysis (Table 4), ²⁰⁶Pb/²⁰⁴Pb of Pb isotopic composition of the alkali basalt from Hadat Tolgoi region is

18.434–18.550, and the value of ²⁰⁷Pb/²⁰⁴Pb is 15.541–15.569, while ²⁰⁸Pb/²⁰⁴Pb is 38.331–38.536. The lead isotopic compositions of whole-rock are stable.

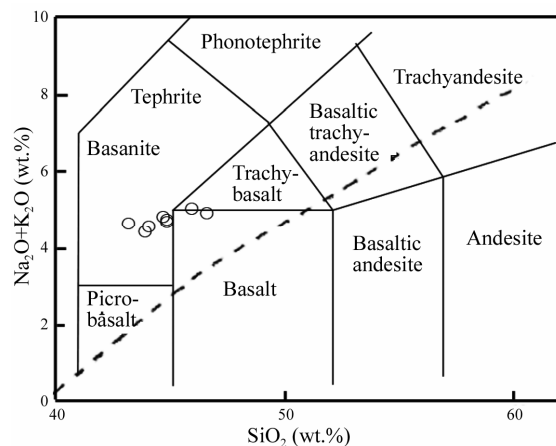


Fig. 4. TAS (after Le Maitre, 1989) diagram for alkali basalts from Hardat Tolgoi Mine.

5 Discussion

5.1 Characteristics of source areas and material sources

Contents of MgO, Cr, and Ni in alkali basalts from Hadat Tolgoi mine are similar to primary magma reference value (MgO=10%–12%, Cr= 250×10^{-6} – 670×10^{-6} , Ni= 90×10^{-6} – 670×10^{-6} , Wendlandt et al., 1995). Mg[#] (55.47–65.47) is also similar with native magma reference value (Mg#=68–75, Frey et al., 1978). It is showed that parent magma may come from primitive mantle magma.

As showed in previous study, basalts which come from asthenosphere typically have the characteristics of La/Nb<1.5 and La/Ta<22, while basalts come from lithosphere are on the contrary (Tompson and Morrison, 1988). La/Nb of alkali basalts from this studying area is 0.56–0.62, and La/Ta is 8.35–9.11. It is showed that it may come from mantle asthenosphere. Although differences in the degree of melting of mantle peridotite can lead to variations of TiO₂ content in basalt, the basaltic magma from the asthenosphere generally has a relatively high Ti content (average value of TiO₂ in OIB's is 2.86%), while Ti content of basaltic magma from the lithosphere mantle is relatively low (Ewart et al., 1998). High TiO₂ content in volcanic rocks (2.95%–3.34%) mainly comes from the asthenosphere mantle. All samples have steep HREE distribution patterns (Fig. 5a), which indicate that the magma comes from a single garnet mantle (Miller et al., 1999).

Table 4 Lead isotopic compositions of the alkali basalts

Sample	$^{206}\text{Pb}/^{204}\text{Pb}$	Std err	$^{207}\text{Pb}/^{204}\text{Pb}$	Std err	$^{208}\text{Pb}/^{204}\text{Pb}$	Std err
09189	18.550	0.003	15.569	0.003	38.536	0.006
09191	18.498	0.003	15.550	0.003	38.430	0.007
09193	18.434	0.004	15.541	0.003	38.331	0.008

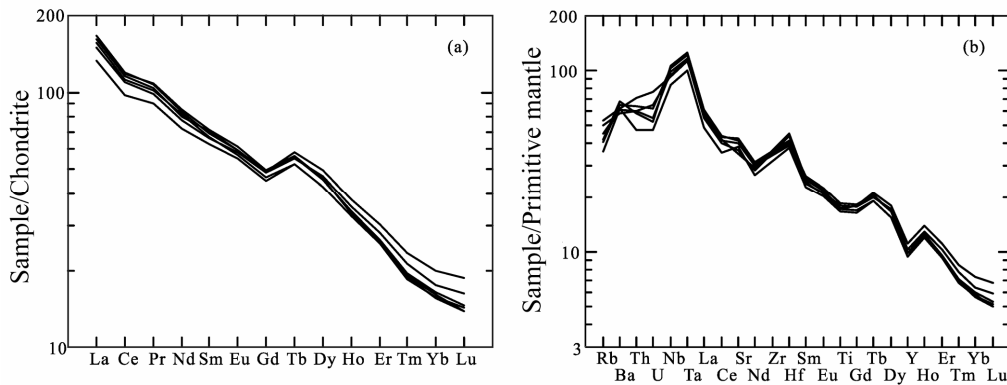


Fig. 5. Chondrite normalized REE patterns (a) and trace element spidergram (b) for the alkali basalts (McDonough and Sun, 1995).

Rb, Sr, Ba and Nb have a high compatibility in the amphibole, while Rb and K have more compatibility in the phlogopite (Adams et al., 1993). Thus, melt generated by hornblende decomposition has a higher content of Ba and higher Ba/Rb and Nb/Th ratios, while the melt phase equilibrated with phlogopite has high Rb/Sr value and low Ba/Rb value (La Tourette et al., 1995). As showed by Ba/Rb-Rb/Sr covariant diagram, Rb/Sr ratio of all samples is high with small variations (Fig. 6), and higher than those for the primitive mantle (Sun and McDonough, 1989). Ba/Rb ratio changes a little and is higher than that in the primitive mantle (Sun and McDonough, 1989). Alkaline basalt could mainly be derived from partial melting of the mantle asthenospheric phlogopite and amphibole. In addition, high Ba contents are more common in disseminated amphibole and mica rather than in these two minerals of vein-shaped in such basalts (Ionov and Griffin, 1997; Schmidt et al., 1999). Therefore, characteristics of Ba enrichment of the alkali basalts may be caused by disseminated phlogopite and amphibole existed in the source region in the mantle.

As showed in Pb isotopic structure model (Fig. 7a), Pb isotopic composition of the alkali basalt from the study area is between those of the mantle and orogenic belts. It is showed that Pb is mainly derived from the mantle. In the $(^{206}\text{Pb}/^{204}\text{Pb})$ - $(^{208}\text{Pb}/^{204}\text{Pb})$ diagram (Fig. 7b), Pb isotopic composition of the alkali basalt from this study projected in mature island arc range, indicating that Pb with the features of mature island arc basalts is mainly derived from the mantle.

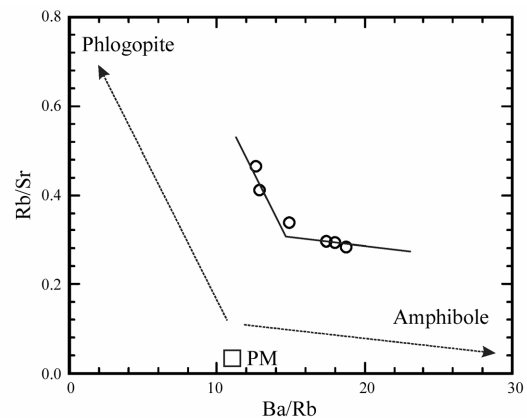


Fig. 6. Covariogram for Ba/Rb vs. Rb/Sr of the alkali basalts (Sun and McDonough, 1989).

5.2 Tectonic environment and crust evolution

Tectonic environment for the formation of these basalts may be implied by trace elements, in particular by incompatible high field strength elements (such as Nb, Ta, Zr, Hf, Ti, and Y). According to Rb/Y-Nb/Y ratio diagrams built by inactive elements during the period of alteration (Pearce, 1982), alkali basalt from Hadat Tolgoi mine can be distinguished as formed in continental rift valley areas (Fig. 8).

The incompatible elements ratio diagrams can reflect elements compositions of the basalt source area. As showed in Ba/La-Ba/Nb diagram (Fig. 9), it is illustrated that some elements of the enriched mantle EM I and EM II can be formed by mantle end-members HIMU mixed with high U/Pb ratios and continental crust materials in different proportions

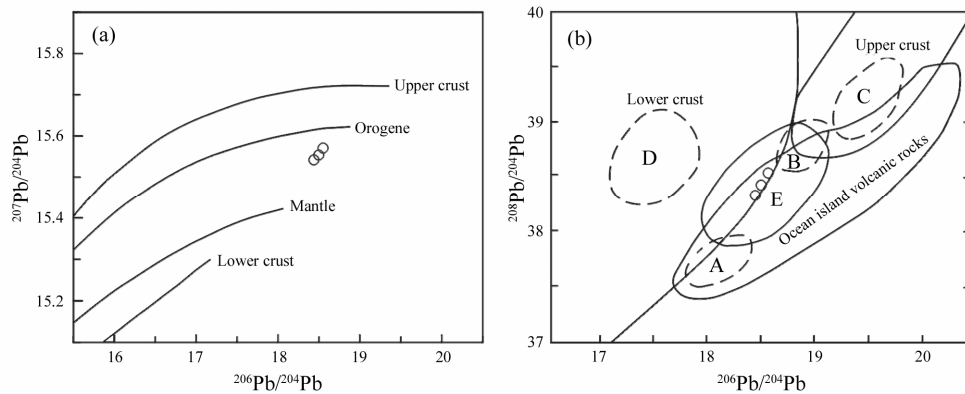


Fig. 7. Plumbotectonic model (a) and $^{206}\text{Pb}/^{204}\text{Pb}$ vs. $^{208}\text{Pb}/^{204}\text{Pb}$ diagram (b) for the alkali basalts (after Zartman and Hart, 1981). A. mid-ocean ridge basalt; B. deep-sea sediment; C. upper crust; D. lower crust; E. mature island arc.

(Weave, 1991). Therefore, mantle source types of the alkali basalts from the study area can be analyzed by using this diagram, and the extent of crust-mantle interaction can be distinguished. Projected points of the alkali basalts from Hadat Tolgoi mine all fall near EMII component area. It is showed that alkali basalt source region is HIMU. It is a mixed product of HIMU and small part of continental crust.

Basaltic magma occurred in intraplate setting is usually enriched in high field strength elements, while basaltic magma which was contaminated by crust, or formed in subduction zone environment is usually enriched in large ion lithophile elements. Thus, if basalt in intraplate tectonic setting came from the enriched mantle or had been contaminated by crust, high field strength elements and large ion lithophile elements may be rich. If the basalt in intraplate tectonic setting contains enriched component, Rb content will be proportional to Nb like $\text{Rb}/\text{Nb}=1$ (Edwards et al., 1991). In the Rb/Y-Nb/Y diagram (Fig. 10), the alkali basalts all projected on the right side of the $\text{Rb}/\text{Nb}=1$ trend line, indicating that compared with Rb (LILE), Nb (HFSE) is relatively sufficient, thus contamination by the continental crust is not obvious. This result is consistent with the result in Fig. 9. The alkali basalts from Hahat Tolgoi mine have not been contaminated obviously by crust materials.

5.3 Petrogenesis

During the period of the Cenozoic (1.18 Ma; Luo and Chen, 1990), depth of the primitive mantle-derived basaltic magma source in north and north-east regions of China is 50–80 km (Deng et al., 1990), and that of the asthenosphere mantle is approximately 55–65 km (Wood, 1979). Depth of top surface of the asthenosphere mantle in study area is about 60 km (Weaver et al., 1991). The alkali basalts distributed in Hadat Tolgoi mine is controlled by NNE-trending and east-west trending fault zones. Under the tensile

structural conditions of eastern China, thickness of the crust has been thinning. Melt was produced at the decompression parts of phlogopite and amphibole as-thenosphere in continental intraplate rift zone environment, and formed basaltic magma. The magma rose quickly through the channel and over flow to the surface, and eventually formed alkali basalt in Hadat Tolgoi mine.

6 Conclusions

(1) The alkali basalts developed in Hadat Talgoi mine is characterized by low silica and high alkali (sodium-rich) and iron titanium contents. The REE patterns show the trend of the "rightist". The fractionation between light and heavy rare earth is obvious, without evidently negative Eu anomaly. LILEs are depleted while the basalts are enriched in HFSEs.

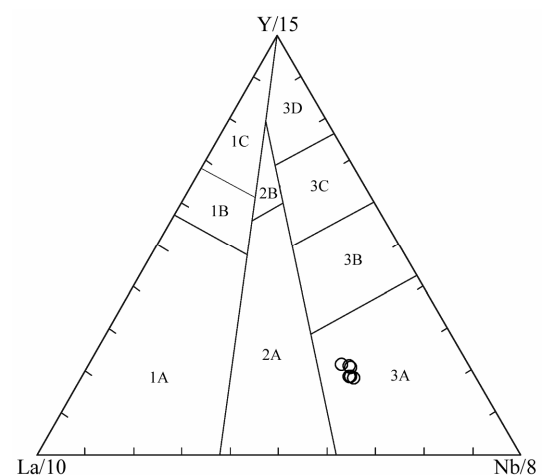


Fig. 8. Y/15-La/10-Nb/8 discrimination diagram for the alkali basalts (Cabani et al., 1989). 1A. Calc-alkaline basalt; 2A. continental basalt; 3A. alkaline basalt in plate rift valley areas; 1B. 1A and 1C overlap areas; 2B. arc basin basalt; 3B. enriched MORB; 1C. volcanic arc tholeiite; 3C. weakly enriched MORB; 3D. normal MORB.

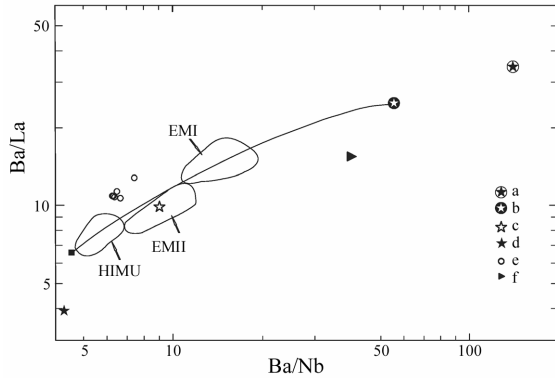


Fig. 9. Ba/La vs. Ba/Nb diagram for the alkali basalts (Weaver et al., 1991). HIMU. Mantle with high μ value; EMI. enriched mantle I; EM II. enriched mantle II; a. average component of lower crust in Southeast China (after Yu et al., 2003); b. average component of world continental crust; c. primitive mantle; d. N-MORB (normal mid-ocean ridge basalt); e. alkali basalts in research area; f. average composition of the exposed crust of Inner Mongolia axis of earth. Curve in the diagram is mixing line of HIMU and materials from the continental crust.

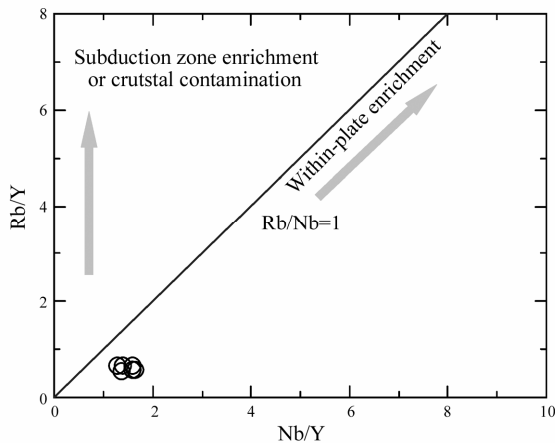


Fig. 10. Rb/Y vs. Nb/Y diagram for the alkali basalts (Temel et al., 1998).

(2) Whole rock Pb isotopic compositions of the alkali basalts in the mine are relatively stable. $^{206}\text{Pb}/^{204}\text{Pb}=18.434\text{--}18.550$, $^{207}\text{Pb}/^{204}\text{Pb}=5.541\text{--}15.569$, and $^{208}\text{Pb}/^{204}\text{Pb}=38.331\text{--}8.536$.

(3) The alkali basalts from Hadate Tolgoi mine were formed in intraplate setting of continent stretching environment. It is the product of rapid rising of the melt derived from decompression partial melting of phlogopite-amphibole bearing material from asthenospheric mantle. The primary magma has not been contaminated significantly by crust materials.

Acknowledgements This study is supported by National Nature Science Foundation of China (No. 40973030). The authors are grateful to Professor Xu Zhaowen of Nanjing University for his thoughtful

review and constructive comment. We appreciate Yang Xiaonan of the Geological Museum of China for his careful corrections of the article.

References

- Adam J.D., Green T.H., and Sie S.H. (1993) Proton Microprobe determined partitioning of Rb, Sr, Ba, Y, Zr, Nb and Ta between experimentally produced amphiboles and silicate melts with variable F content [J]. *Chemical Geology*. **109**, 29–49.
- Cabanis B. and Lecolle M. (1989) Le digramme La/10-Y/15-Nb/8: un outil pour la discrimination de series volcaniques et la mise en evidence des processus de melange et/ou de contamination crustale [J]. *CR Academic Science Series II*. **309**, 2023–2029.
- Chen Jinquan, Xu Zhaowen, Bai Kangchen, Chen Wei, Wang Hao, and Wang Shaohua (2012) The petrochemistry of the diabase from the Hardat Tolgoi Pb-Zn Minefield, Inner Mongolia [J]. *Geotectonica et Metallogenia*. **36**, 118–126 (in Chinese with English abstract).
- Deng Jinfu and Zhao Hailing (1990) In *Nature of Upper Mantle and Dynamics in China* [C]. pp.8–13. Seismic Publishing House, Beijing (in Chinese).
- Edwards C., Menzies M., and Thirlwall M. (1991) Evidence from Muriah, Indonesia, for the interplay of supra-subduction zone and intraplate processes in the genesis of potassic alkaline magmas [J]. *Journal of Petrology*. **32**, 555–592.
- Ewart A., Milner S.C., Armstrong R.A., and Dungan A.R. (1998) Etendeka volcanism of the Goboboseb Mountains and Messum igneous complex, Namibia. Part I: Geochemical evidence of Early Cretaceous Tristan Plume Melts and the role of crustal contamination in the Paraná–Etendeka CFB [J]. *Journal of Petrology*. **39**, 191–225.
- Frey F.A., Green D.H., and Roy S.D. (1978) Integrated models of basalt petrogenesis: A study of quartz tholeiites to olivine melilitites from south eastern Australia utilizing geochemical and experimental petrological data [J]. *Journal of Petrology*. **19**, 463–513.
- Gao Jianfeng, Lu Jianjun, Lai Mingyuan, Lin Yuping, and Pu Wei (2003) Analysis of trace elements in rock samples using HR-ICPMS [J]. *Journal of Nanjing University (Natural Sciences)*. **39**, 844–850 (in Chinese with English abstract).
- Irvine T.N. and Baragar W.R.A (1971) A guide to the chemical classification to the common volcanic rocks: Canada [J]. *Journal of Earth Science*. **8**, 523–548.
- Ionov D.A., O'Reilly S.Y., and Griffin W.L. (1997) Volatile bearing minerals and lithophile trace elements in the upper mantle [J]. *Chemical Geology*. **141**, 153–184.
- LaTourette T., Hervig R.L., and Holloway J.R. (1995) Trace element partitioning between amphibole, phlogopite, and basanite melt [J]. *Earth Planetary Science Letters*. **135**, 13–30.
- Le Maitre R.W., Bateman P., and Dudek A. (1989) *A Classification of Igneous Rocks and Glossary of Terms* [M]. Oxford, Blackwell.
- Li Changnian (1992) *Igneous Rock Trace Element Petrology* [M]. pp.79–123. China University of Geoscience Press, Wuhan (in Chinese).
- Liu Yikang and Xu Yebing (2003) The prospecting and main Features of Oyu Tolgol porphyry Cu-Au deposit in Mongdia [J]. *Geology and Prospecting*. **39**, 1–4 (in Chinese with English abstract).

- Luo Xiuquan and Chen Qitong (1990) Preliminary study on geochronology for Cenozoic basalts from Inner Mongolia [J]. *Acta Petrologica et Mineralogica*. **9**, 37–46 (in Chinese with English abstract)
- McDonough W.F. and Sun S.S. (1995) The composition of the Earth [J]. *Chemical Geology*. 120,223-254.
- Nie Fengjun, Jiang Sihong, Zhang Yi, Liu Yan, and Hu Peng (2004) Geological features and origin of porphyry copper deposits in China-Mongolia border region and its neighboring areas [J]. *Mineral Deposits*. **23**, 176–189 (in Chinese with English abstract).
- Pearce J.A. (1982) Trace element characteristics of lavas from destructive plate boundaries. In: *Orogenic andesites and related rocks* (ed. Thrope R.S.) [C]. pp.528–548. John Wiley and Sons, Chichester, England.
- Schmidt K.H., Bottazzi P., Vannucci R., and Mengel K. (1999) Trace element partitioning between phlogopite, clinopyroxene and leucite lamproite melt [J]. *Earth and Planetary Science Letters*. **168**, 287–299.
- Sun S.S. and McDonough W.F. (1989) *Chemical and isotopic systematics of oceanic basalts: Implications for mantle composition and processes*. [C] pp.313–345. In *Magmatism in the Ocean Basins* (eds. Saunders A.D. and Norr M.J.) Geol. Soc. London Spec. Publ.
- Temel A., Gündođdu M.N., and Gourgaud A. (1998) Petrological and geochemical characteristics of Cenozoic high-K calc-alkaline volcanism in Konya, Central Anatolia, Turkey [J]. *Journal of Volcanology and Geothermal Research*. **85**, 327–354.
- Thompson R.N. and Morrison M.A. (1988) Asthenospheric and lower-lithospheric mantle contributions to continental extensional magmatism: An example from the British Tertiary province [J]. *Chemical Geology*. **68**, 1–15.
- Wang Xuezhen, Li Yuqin, Zhang Xizhou, Wang Zhensheng, Nie Xiuli, and Li Hongchao. (2010) A preliminary study of the geology and ore potentiality of Hardat Tolgoi Ag-Pb Deposit, Inner Mongolia [J]. *Mineral Exploration*. **1**, 446–452 (in Chinese with English abstract).
- Weaver B.L. (1991) The origin of ocean island basalt end-member composition: Trace element and isotopic constrains [J]. *Earth and Planetary Science Letters*. **104**, 381–397.
- Wendlandt R.F., Altherr R., Nuemann E.R., and Baldrige W.S. (1995) In *Petology, Geochemistry, Isotopes* (ed. Olsen K.H.). [C] pp.47–60. Continental Rifts: Evolution, Structures, Tectonics, Amsterdam: Elsevier.
- Wood J.M. (1979) A variably veined suboceanic upper mantle genetic significance for mid-ocean ridge basalt from geochemical evidence [J]. *Geology*. **7**, 499–503.
- Zartman R.E. and Doe B.R. (1981) Plumbo tectonics the model [J]. *Tectonophysics*. **75**, 135–162.
- Zhang Chen, Han Baofu, Tong Ying, and Li Dechun (2004) General characteristics and origin of Cenozoic basalt from Abagaqi region, Inner Mongolia [J]. *Journal of Jilin University (Earth Science Edition)*. **34**, 21–26 (in Chinese with English abstract).
- Zhang Chen, Liu Shuwen, Han Baofu, and Li Dechun (2006) Characteristics of ultramafic xenoliths from Cenozoic basalts in Abagaqi area, Inner Mongolia [J]. *Acta Petrologica Sinica*. **22**, 2801–2807 (in Chinese with English abstract).
- Zhang Xizhou (2010) Geophysical characteristics of Hardat Tolgoi Ag-Pb deposit, Inner Mongolia [J]. *Mineral Exploration*. **1**, 479–482 (in Chinese with English abstract).
- Zhang Xizhou (2009) *Geological Exploration Report of Hardat Tolgoi Lead-zinc Deposit, Inner Mongolia* [R]. (in Chinese).
- Zhang Yi, Nie Fengjun, Jiang Sihong, and Hu Peng (2003) Discovery of the Ouyu Tolgoi copper-gold deposit in the Sino-Mongolia border region and its significance for mineral exploration [J]. *Geological Bulletin of China*. **22**, 708–712 (in Chinese with English abstract).